

---

# Active Learning with Expected Error Reduction

---

**Stephen Mussmann\***

University of Washington

mussmann@cs.washington.edu

**Julia Reisler\***

Stanford University

jreisler@stanford.edu

**Daniel Tsai**

Apple

daniel\_tsai@apple.com

**Ehsan Mousavi**

Apple

emousavi@apple.com

**Shayne O'Brien**

Apple

shayne\_obrien@apple.com

**Moises Goldszmidt**

Apple

mgoldszmidt@apple.com

## Abstract

Active learning has been studied extensively as a method for efficient data collection. Among the many approaches in literature, Expected Error Reduction (EER) Roy & McCallum (2001) has been shown to be an effective method for active learning: select the candidate sample that, in expectation, maximally decreases the error on an unlabeled set. However, EER requires the model to be retrained for every candidate sample and thus has not been widely used for modern deep neural networks due to this large computational cost. In this paper we reformulate EER under the lens of Bayesian active learning and derive a computationally efficient version that can use any Bayesian parameter sampling method (such as Gal & Ghahramani (2016)). We then compare the empirical performance of our method using Monte Carlo dropout for parameter sampling against state of the art methods in the deep active learning literature. Experiments are performed on four standard benchmark datasets and three WILDS datasets (Koh et al., 2021). The results indicate that our method outperforms all other methods except one in the data shift scenario – a model dependent, non-information theoretic method that requires an order of magnitude higher computational cost (Ash et al., 2019).

## 1 Introduction

Active learning studies how adaptivity in data collection can decrease the data requirement of machine learning systems (Settles, 2009) and has been applied to a variety of applications such as medical image analysis where unlabeled samples are plentiful but labeling via annotation or experimentation is expensive. In such cases, intelligently selecting samples to label can dramatically reduce the cost of creating a training set. A range of active learning algorithms have been proposed in recent decades (Lewis & Gale, 1994; Tong & Koller, 2001; Roy & McCallum, 2001). Current research trends have shifted towards active learning for deep learning models (Sener & Savarese, 2018; Ash et al., 2019; Gal et al., 2017; Sinha et al., 2019), which present a new set of constraints that traditional methods do not always address.

Another application of active learning has been in addressing data shift (Rabanser et al., 2019; Schrouff et al., 2022), a problem which can be summarized as deploying a model to a distribution that is different from the training distribution, and is characteristic of real world machine learning applications. This is a critical aspect of model deployment because distributional shifts can cause significant degradation in model performance. Active learning has been proposed as a method to mitigate the effects of data shift by identifying salient out-of-distribution samples to add to the training data (see, for example, Kirsch et al. (2021) and Zhao et al. (2021)).

---

\*Work done while at Apple

In this paper we propose a new derivation of the Expected Error Reduction (EER) active learning method (Roy & McCallum, 2001) and apply it to deep neural networks in experiments with and without data shift, expanding upon the original setting of simple classifiers such as Naive Bayes. At its core, EER chooses a sample that maximally reduces the generalization "error" or "loss" in expectation. The original implementation of EER requires retraining the classifier model for every possible candidate sample, for every possible label. The cost of this constant retraining is intractable in the deep neural network context. To circumvent this, we present a formulation that estimates the value of a label for reducing the classifier's loss without retraining the neural network. We achieve this by casting EER in the context of Bayesian methods and drawing samples from the model posterior conditioned on the data. Although sampling from the Bayesian posterior of model parameters directly can be difficult, there are a variety of methods to approximate this distribution such as Monte Carlo dropout (Gal & Ghahramani, 2016), ensembles (Beluch et al., 2018), and Langevin dynamics (Welling & Teh, 2011).

Perhaps the earliest Bayesian data collection method is Expected Information Gain (Lindley, 1956) which is equivalent to selecting the sample with the label that has the highest mutual information with the model parameters. This method has been explored by Gal et al. (2017) for active learning in the context of deep neural networks, and is referred to as BALD. While BALD maximizes the information encoded by model parameters about the dataset, the fundamental goal of classification is to identify the model parameters that minimize test error. This imperfect alignment in the objective is what motivates our exploration of EER. Similar to Roy & McCallum (2001), we consider two variants of the method: one based on zero-one loss, which we refer to as minimization of zero-one loss (MEZL), and the other on log-likelihood loss, which we refer to as minimization of log-likelihood loss (MELL). Our derivation also enables us to cast EER in an information theoretic setting that allows for a theoretical comparison with BALD. Both BALD and MELL reduce the epistemic uncertainty, but MELL additionally removes task irrelevant information (see 3.3). We hypothesize that this explains why MELL outperforms BALD empirically (see Section 4.2).

In our experiments we compare MELL and MEZL against state of the art active learning methods including BADGE (Ash et al., 2019), BALD (Gal et al., 2017), and Coreset (Sener & Savarese, 2018) on seven image classification datasets. For each dataset, we perform experiments in both a setting with and without data shift. We remark that unlike the work of Kirsch et al. (2021) where the goal is to avoid labeling out of distribution samples, we are interested in the realistic scenario of reducing model error on a test set that may be drawn from a different distribution than the seed set. In our results, MELL consistently performs better or on par with all other approaches in both the no data shift and data shift settings, with the largest gains above BALD coming in the data shift setting.

The only approach that compares favorably to ours is BADGE, which outperforms MELL and MEZL on two datasets under data shift: Camelyon17 and MNIST. However, MELL and MEZL require orders of magnitude less computation cost (see Section 4.2 and Appendix A.2) and are model agnostic – they can be applied to neural networks, random forests, linear models, etc. We also remark that optimizing the log likelihood (MELL) performs better than zero-one loss objective (MEZL) (see Section 5 for an explanation).

In summary, the contributions of this paper are:

1. A Bayesian reformulation of the EER framework to enable computational efficiency with deep neural networks.
2. An empirical evaluation of the effectiveness of the proposed method, comparing it to other state of the art deep active learning approaches on seven datasets, each with and without data shift.

We introduce our active learning setting in Section 2 before deriving our method in Section 3. Next, we provide an empirical evaluation in Section 4. Finally, we discuss the implications, context, and related work in Section 5 and conclude with Section 6.

## 2 Setting

We study a classification setting where we have an input space  $\mathcal{X}$  and a discrete label space  $\mathcal{Y} = [C] = \{1, \dots, C\}$ . We wish to find a function  $f : \mathcal{X} \rightarrow \mathcal{Y}$  such that the misclassification error (zero-one loss),  $\mathbb{E}_{(x,y)}[f(x) \neq y]$ , is small according to some data distribution.

In this paper we consider pool-based active learning where there is an “unlabeled” pool  $\mathcal{D}_{\text{pool}}$  drawn from some distribution  $D_{\text{target}}$  where the labels of the samples are hidden. In each of the  $K$  iterations, an active learning algorithm chooses  $n_{\text{query}}$  samples from  $\mathcal{D}_{\text{pool}}$ , the labels are revealed, and the samples are added to the training set. Often, active learning algorithms calculate a score for each sample and choose to query the set of  $n_{\text{query}}$  unlabeled samples with the highest scores. We consider two settings for the initial training set  $\mathcal{D}_{\text{seed}}$ : when it is not sampled from  $D_{\text{target}}$ , and when it is sampled from  $D_{\text{target}}$ . We refer to these scenarios as active learning with and without “data shift” respectively. In both cases, we evaluate on samples from  $D_{\text{target}}$ .

We take the Bayesian perspective that the model parameters  $\theta$  are a random variable drawn from a known prior. As is typical, we assume that the labels of samples are conditionally independent given  $\theta$ . At a given iteration, let  $\mathcal{D}$  be the labeled data collected thus far and  $\Pr(\theta|\mathcal{D})$  be the posterior. We view the remaining unlabeled pool  $\{x_i\}$  as fixed but the labels as random variables  $\{Y_i\}$ .

### 3 Method

The guiding principle of our reformulation of EER is to score a candidate sample by the expected reduction in loss if we sampled the candidate’s label. In this section, we provide a formalization of this idea that only requires the pairwise marginals for the labels. These marginals can be approximated in a computationally efficient way using Bayesian sampling methods such as Monte Carlo dropout (Gal & Ghahramani, 2016).

Candidates for labeling are selected from  $\mathcal{D}_{\text{pool}}$ . Additionally, we assume access to a small secondary set of unlabeled data for validation  $\mathcal{D}_{\text{val}}$ , which is used for the evaluation of the expected loss reduction. Note that we do not assume that the two sets  $\mathcal{D}_{\text{pool}}$  and  $\mathcal{D}_{\text{val}}$  are drawn from the same distributions. In contrast, Roy & McCallum (2001) use the same set for both validation and pool of candidates. This distinction affords us more flexibility, especially in the data shift case.

Because retraining a deep neural network for every candidate sample is computationally infeasible, our aim is to approximate the expected reduction in error. We use Bayesian sampling to approximate the effect of observing the label for every candidate sample on the error over the validation dataset and add the candidate and label that precipitates the highest reduction in error to the training set. We formalize this in Equation 1 below. The  $\text{Score}_i$  is the difference between two terms: the first term represents the total sum of the expected loss over  $\mathcal{D}_{\text{val}}$ , and the second term estimates the expected loss over  $\mathcal{D}_{\text{val}}$  when we fix the label of the candidate sample  $i$ . Although we do not know the ground truth label of the candidate sample, we can take the expectation with respect to the posterior to compute an approximation for each possible label. The probabilities in the equation below are implicitly conditioned on samples from the validation set  $\{x_1, \dots, x_{n_{\text{val}}}\}$  and on the candidate sample  $x_i$ .

$$\text{Score}_i = \sum_{j=1}^{n_{\text{val}}} \min_{a \in \mathcal{A}} \mathbb{E}_{y_j \sim Y_j | \mathcal{D}} [\ell(y_j, a)] - \mathbb{E}_{y_i \sim Y_i | \mathcal{D}} \left[ \sum_{j=1}^{n_{\text{val}}} \min_{a \in \mathcal{A}} \mathbb{E}_{y_j \sim Y_j | \mathcal{D}, Y_i = y_i} [\ell(y_j, a)] \right] \quad (1)$$

Here,  $a$  represents the optimal prediction (relative to a particular probability distribution),  $\mathcal{A}$  is the set of possible predictions, and  $\ell$  is the loss. Note that the first term in Equation 1 is constant with respect to the samples of  $\mathcal{D}_{\text{pool}}$ , and thus does not have any effect on comparing samples. Thus Equation 2 is a reduced form where we estimate the score based solely on the second term; the negation of the expected loss on  $\mathcal{D}_{\text{val}}$  after the estimating the candidate sample’s label.

$$\text{Score}_i = -\mathbb{E}_{y_i \sim Y_i | \mathcal{D}} \left[ \sum_{j=1}^{n_{\text{val}}} \min_{a \in \mathcal{A}} \mathbb{E}_{y_j \sim Y_j | \mathcal{D}, Y_i = y_i} [\ell(y_j, a)] \right] \quad (2)$$

Throughout the remainder of this work, we will continue to use  $i$  and  $j$  to index samples in  $\mathcal{D}_{\text{pool}}$  and  $\mathcal{D}_{\text{val}}$  respectively and omit the conditioning on  $\mathcal{D}$ ,  $\{x_1, \dots, x_{n_{\text{val}}}\}$ , and  $x_i$  for brevity.

We remark on the following aspects of our definition of EER ( $\text{Score}_i$ ):

- Because we focus on a Bayesian approach, we are able to sidestep the model retraining requirement in EER and work with expectations. Appendix A.1 shows that only the quantities  $\Pr(Y_i = y_i)$  and  $\Pr(Y_j = y_j | Y_i = y_i)$  are needed.

- In Equation 2, the loss is computed with respect to the validation set  $\mathcal{D}_{\text{val}}$  (note that the ground truth labels for the validation set are not used). This affords additional flexibility in case the  $\mathcal{D}_{\text{pool}}$  samples are not drawn from the *target distribution*.

In the next subsections, we derive criteria for two different losses: the negative log-likelihood loss (MELL) and the zero-one loss (MEZL).

### 3.1 MELL

To obtain the expression for MELL, we substitute the general loss,  $\ell(y_j, a)$ , for the (negative) log-likelihood loss,  $-\log a_{y_i}$ , into Equation 2. For the log-likelihood loss, the set of possible predictions is the probability simplex over the  $C$  classes,  $\mathcal{A} = \Delta_C$ , and thus  $a_{y_i}$  is the vector  $\Pr(Y_i|x_i, D)$ . We use the non-negativity of the KL divergence to find the optimal prediction for each  $a_{y_i}$  as  $\Pr(Y_j = \cdot | Y_i = y_i)$  (see the proof in Appendix A.1), and by the definition of conditional entropy we obtain the succinct expression,  $\text{Score}_i = -\sum_{j=1}^{n_{\text{val}}} H(Y_j|Y_i)$ , where  $H(\cdot|\cdot)$  is the conditional entropy. Using  $H(Y_j|Y_i) = H(Y_j, Y_i) - H(Y_i)$  yields the final expression:

$$\text{Score}_i = n_{\text{val}}H(Y_i) - \sum_{j=1}^{n_{\text{val}}} H(Y_j, Y_i). \quad (3)$$

To estimate these quantities we need to compute  $\Pr(Y_i = c)$  and  $\Pr(Y_i = c, Y_j = c')$ . Because the parameters  $\theta$  render the labels conditionally independent, we can draw  $T$  samples from the posterior as  $\{\theta_t\}_{t=1}^T$  and perform the following unbiased Monte Carlo approximation of these probabilities:

$$\Pr(Y_i = c) \approx \frac{1}{T} \sum_{t=1}^T \Pr(Y_i = c|\theta_t) \quad (4)$$

$$\Pr(Y_i = c, Y_j = c') \approx \frac{1}{T} \sum_{t=1}^T \Pr(Y_i = c, Y_j = c'|\theta_t) = \frac{1}{T} \sum_{t=1}^T \Pr(Y_i = c|\theta_t) \Pr(Y_j = c'|\theta_t), \quad (5)$$

Sampling parameters from the *posterior distribution* can be approximately generated in a variety of ways. In our implementation, we use *Monte Carlo dropout* for its computational efficiency. Another approximate method is *Cyclical SG-MCMC*, proposed in Zhang et al. (2019). In our experiments we find that *Monte Carlo dropout* performs better empirically than *Cyclical SG-MCMC* (see Figure 4 in Appendix A.4.2).

### 3.2 MEZL

For the zero-one loss we substitute the general loss,  $\ell(y_j, a)$ , for  $\mathbf{1}[y_j \neq a]$  into Equation 2, where the set of possible predictions is simply the output set  $\mathcal{Y} = [C]$  and the optimal prediction for  $a$  is  $\arg \max_{c \in [C]} \Pr(Y_j = c|Y_i = y_i)$ . Then using some algebra, we obtain

$$\text{Score}_i = \sum_{c \in [C]} \sum_{j=1}^{n_{\text{val}}} \max_{c' \in [C]} \Pr(Y_j = c', Y_i = c) - n_{\text{val}}. \quad (6)$$

We can ignore the  $n_{\text{val}}$  term since it remains constant with respect to  $i$ . Like MELL, the MEZL criteria requires knowing the pairwise marginals of the labels which can be estimated using Monte Carlo methods and the conditional independence of the labels given the parameters, as in Equation 5.

### 3.3 Information decomposition

As before, let  $Y_i$  be the label of a sample  $x_i$  in  $\mathcal{D}_{\text{pool}}$  and  $Y_j$  be the label of a sample  $x_j$  in  $\mathcal{D}_{\text{val}}$ .  $\theta$  is the random variable for the posterior distribution of the parameters. Using an information-theoretic

identity, the total uncertainty  $H(Y_i)$  of a sample in the pool can be decomposed into the epistemic uncertainty and the aleatoric uncertainty, namely  $H(Y_i) = I(Y_i; \theta) + H(Y_i|\theta)$ .

Because we cannot reduce the aleatoric uncertainty  $H(Y_i|\theta)$ , BALD judiciously minimizes the epistemic uncertainty rather than the total uncertainty. There is a similar decomposition of the mutual information  $I(Y_i; \theta)$  into the interaction information  $I(Y_j; Y_i; \theta)$  and the conditional mutual information  $I(Y_i; \theta|Y_j)$ . Although the interaction information can in general be negative, the assumption that the labels are conditionally independent given the parameters implies that  $I(Y_j; Y_i; \theta) = I(Y_j; Y_i) \geq 0$ . Thus,

$$I(Y_i; \theta) = I(Y_i; Y_j; \theta) + I(Y_i; \theta|Y_j) \quad (7)$$

$$= I(Y_i; Y_j) + I(Y_i; \theta|Y_j). \quad (8)$$

Intuitively,  $I(Y_i; \theta|Y_j)$  is the information that is irrelevant to the prediction of the validation sample  $Y_j$ . The term  $I(Y_i; Y_j)$  is then the only relevant information. Note that if we take the score of a pool sample  $i$  as the sum of the task-relevant information with respect to all validation samples, we recover MELL. Hence MELL can be seen as an algorithm like BALD, after removing the information that is not relevant to a validation set.

In Appendix A.6, we look more closely at these terms for the case of a linear Bayesian model. We show that the irrelevant information term (second term) in decomposition 7 dominates the BALD sampling objective and thus samples with the largest norm are selected. In contrast, MELL focuses on the samples with larger impact on the validation set.

## 4 Experiments

### 4.1 Setup

We experiment with active learning on 7 image classification datasets – CIFAR10, CIFAR100, SVHN, MNIST, Camelyon17, iWildCam, and FMoW – each in a setting of data shift and no data shift, for a total of 14 experiments.

Each experiment follows the standard active learning setup as described in Section 2. In the no shift setting, there is no distribution shift between seed, pool, test, and validation sets. In the shift setting, pool, test, and validation come from the same distribution, while seed is from a different distribution. Please refer to Appendix A.3.2 for more details about the datasets and how shifts were induced in each. Section A.3.3 details the experimental parameters.

We compare MELL and MEZL to several existing methods in the literature that are representative of the state of the art in active learning. We use **Random**, consisting of uniform random sampling from the pool as a baseline. We compare to three information-theoretic methods: **BALD** (Gal et al., 2017), where the candidates are scored by their mutual information with the parameters  $I(Y_i; \theta)$  estimated using Monte Carlo dropout; **Entropy\_MC** (Lewis & Gale, 1994), which relies on entropy-based uncertainty sampling using probabilities from Monte Carlo dropout; and **Entropy**, which also relies on entropy-based uncertainty sampling, this time using probabilities from the softmax output. The formal relation of these methods to MELL was detailed in Section 3.3. In addition, we also compare against two empirically successful methods based on diversity sampling approaches that require access to the last layer of the task model (not model-free). The first one is **Coreset** (Sener & Savarese, 2018), which relies on batch sampling a group which provides representative coverage of the unlabeled pool using the penultimate layer representation. We remark that that our experimental results for **Coreset** are generated using a greedy approximation of the method for computational efficiency. The second one is **BADGE** (Ash et al., 2019), which chooses samples that are diverse and high-magnitude when represented in a hallucinated gradient space with respect to model parameters in the final layer. The scoring functions for these methods can be found in Section A.3.1

### 4.2 Results

Our experiments find that MELL is the best performer or tied with best on 12 out of the 14 experiments, suggesting that MELL performs well across a variety of domains. According to Table 1, MELL never

Table 1: Comparison between MELL and baseline methods based on the AUC of the active learning accuracy curves. A method wins against another method if the mean AUC - standard deviation is above the other method’s mean AUC + standard deviation. Otherwise, there is tie. Note that **BADGE** only finished running for 9 experiments.

	BADGE	BALD	Coreset	Entropy_MC	Entropy	MEZL	Random
MELL wins	0	4	3	6	7	2	10
MELL ties	7	10	11	8	6	12	4
MELL losses	2	0	0	0	1	0	0

performs worse than BALD and Coreset, outperforming BALD on 4 experiment and Coreset on 3. We show the active learning curves for the experiments where MELL outperformed BALD or Coreset in Figure 1.

For the cases where MELL outperforms BALD, we find that the performance gap is particularly wide for the data shift cases. We believe this is because BALD selects samples which maximize the information gain about the model posterior, which may not be particularly helpful for the target distribution, whereas MELL selects samples with the specific criteria of reducing error on the target distribution.

In the case of data shift (see Table 5), we have two exceptions: in MNIST, **BADGE** outperforms MELL, and in Camelyon17 both **BADGE** and **Entropy** outperform MELL. We first note that **Entropy** under-performs with respect to MELL in 7 other settings. **BADGE** on the other hand, performs on par with MELL in all the cases where the computation finishes. For iWildCam and FMoW, the computations required by **BADGE** didn’t finish after 14 days of execution. Indeed, **BADGE** achieves its performance at a steep cost in terms of computation time. Figure 2 shows the exact cost for the case of Camelyon17 with shift. Note that most of the overhead is on the active learning method itself and not on the training of the task model. This behavior is consistent in all of the experiments. We offer some further insight in terms of computational complexity in Appendix A.2.

In addition, we point out that it has been noted that Camelyon17 is an outlier among datasets. From Miller et al. (2021): “One possible reason for the high variation in accuracy [on Camelyon17] is the correlation across image patches. Image patches extracted from the same slides and hospitals are correlated because patches from the same slide are from the same lymph node section, and patches from the same hospital were processed with the same staining and imaging protocol. In addition, patches in [Camelyon17] are extracted from a relatively small number of slides.” Because of this test time dependence between images (in addition to train time dependence), Miller et al. (2021) notes the presence of “instabilities in both training and evaluation”.

MEZL performs on par with random selection or significantly underperforms the best methods on MNIST, CIFAR10, SVHN, and Camelyon17. This underperformance is due to the fact that MEZL is only sensitive to validation samples that are near the decision boundary. A further discussion of this phenomenon is in Section 5.1.

To summarize, we find that MELL outperforms or is comparable to existing state of the art methods for active learning in a variety of situations. There is no other method that performs consistently in all scenarios at the same level of computational efficiency. Our experiments hint that MELL may be appropriate for a wide range of tasks and might partially eliminate the need to make a decision about which active learning method to use. Active learning accuracy curves for all experiments and tables containing the AUCs of these experiments can be found in Appendix A.4.1.

## 5 Discussion

A result of the information theoretic basis of our scores, plus the use of Bayesian estimates, is that the only requirement for the computation of MELL and MEZL is the estimation of the pairwise marginal probabilities of labels. Thus, these scores can be applied to deep neural networks, random forests, linear models, etc., with very little modification. This clearly contrasts with methods such as Coreset and **BADGE** which make use of the last-layer activation of the neural network. In that precise sense, our approach is *model free*.

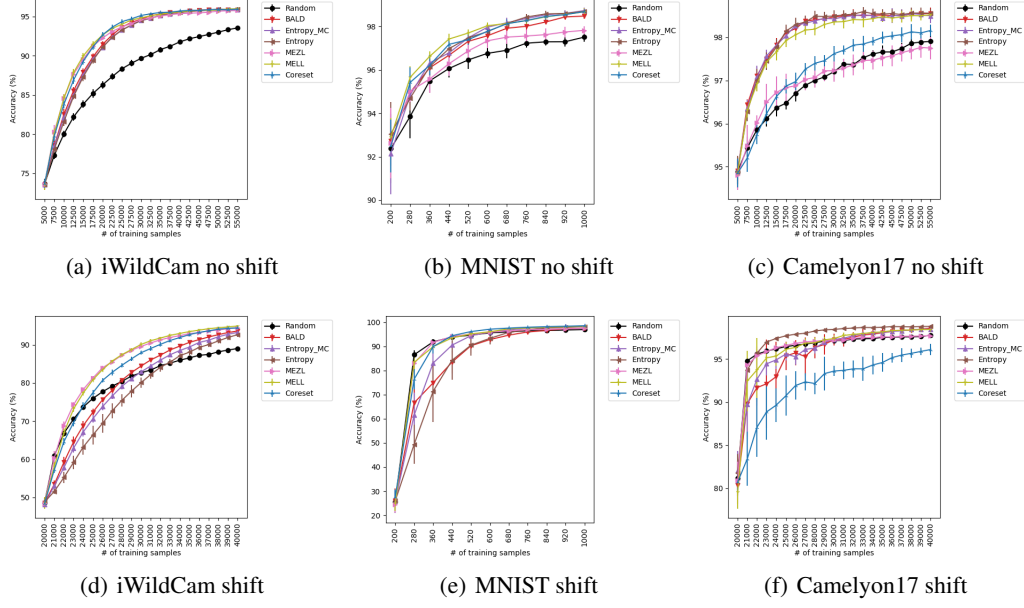


Figure 1: The accuracy curves over the test set on MNIST, Camelyon17, and iWildCam under shift and no shift settings. MELL outperforms BALD on iWildCam and MNIST in both settings. MELL outperforms Coreset on Camelyon17 in both settings and iWildCam with shift.

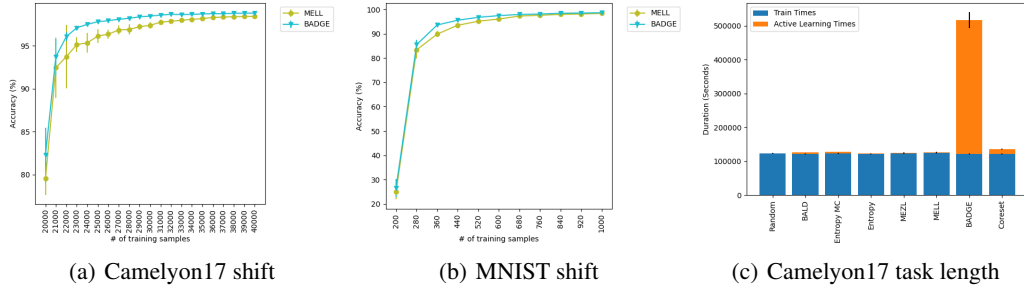


Figure 2: (a) Accuracy curves and (b) total amount of time for MELL and BADGE on Camelyon17 with shift. The total time is averaged over 10 trials for each active learning strategy, and the black error bars represent the standard deviation.

In addition, we characterized the differences between (a) entropy-based uncertainty sampling, (b) the expected information gain score (BALD), and (c) minimization of expected log-likelihood loss (MELL), in a precise information-theoretic light that explains the formal relationship between these methods. We remark that these methods are myopic in the way they score each sample independent of the others and greedily rank the outcomes. In Appendix A.5, we discuss the possibility of extending MELL to a non-myopic algorithm.

An important difference between our work and the original EER framework is that we make use of an unlabeled validation set rather than relying on the unlabeled pool of samples. When there is no data shift, this is a small difference. Knowledge of the labels of the validation set is not required, and we could create the validation set by subsampling the unlabeled pool before the algorithm runs. However, in settings where the unlabeled pool is from a different distribution than the test set and we don't have label access to or much data in the test set, this is an important distinction. It affords us the flexibility to focus the scoring function at a specific set, with the expectation that the algorithm will specialize to the implicit distribution in that set.

### 5.1 Failure mode of MEZL

MEZL performs significantly worse than MELL on some datasets because MEZL is only sensitive to validation samples near the decision boundary. More precisely, if observing the candidate label  $Y_i$  does not change the prediction  $Y_j$  on a validation sample, then the zero-one loss reduction is 0.

$$\text{LossReduction} = \sum_{j=1}^{n_{\text{val}}} \min_{a \in [C]} \mathbb{E}_{y_j \sim Y_j} [\mathbf{1}[y_j \neq a]] - \mathbb{E}_{y_i \sim Y_i} \left[ \sum_{j=1}^{n_{\text{val}}} \min_{a \in [C]} \mathbb{E}_{y_j \sim Y_j | Y_i = y_i} [\mathbf{1}[y_j \neq a]] \right].$$

If the prediction  $a$  does not depend on the value  $y_i$ , then we can bring the expectation of  $Y_i$  inside the  $\min_{a \in [C]}$ . Then, by the law of total expectation, the two terms are equal and there is no reduction in the zero-one loss on label  $j$ . Intuitively, this is a problem because observing some candidates in the pool could increase the confidence on many validation samples without necessarily changing the prediction of any of these samples. These candidates would be regarded as useless by MEZL, although they are useful *in the long term* since reducing uncertainty over several iterations can reduce zero-one loss. Perhaps counter-intuitively, directly minimizing the next-step expected negative log-likelihood loss yields lower zero-one loss over many steps than directly minimizing the next-step zero-one loss.

## 6 Conclusion

In this work, we re-examine the EER algorithm (Roy & McCallum, 2001) from a Bayesian and information theoretic perspective. Our method avoids the requirement of frequent model retraining, required in the original algorithm, which is infeasible in current deep learning models. Instead we make use of estimation techniques such as dropout that make Bayesian active learning strategies computationally efficient. Empirically, the algorithms we propose are effective on standard benchmark datasets against state of the art methods in the literature.

We performed experiments with datasets under conditions of data shift, which have not been thoroughly examined in the active learning literature. We remark that the proper examination of active learning in conditions of shift demands further study. In particular, there are a variety of questions related to designing and adapting active learning methods to the data shift setting that take advantage of the information afforded by the validation sets. We leave these questions for future research, having established results in this work as initial benchmarks.

## References

Ash, J. T., Zhang, C., Krishnamurthy, A., Langford, J., and Agarwal, A. Deep batch active learning by diverse, uncertain gradient lower bounds. [arXiv preprint arXiv:1906.03671](#), 2019.

Bandi, P., Geessink, O., Manson, Q., Van Dijk, M., Balkenhol, M., Hermsen, M., Bejnordi, B. E., Lee, B., Paeng, K., Zhong, A., et al. From detection of individual metastases to classification of lymph node status at the patient level: the camelyon17 challenge. [IEEE transactions on medical imaging](#), 38(2):550–560, 2018.

Beery, S., Cole, E., and Gjoka, A. The iwildcam 2020 competition dataset, 2020.

Beluch, W. H., Genewein, T., Nürnberg, A., and Köhler, J. M. The power of ensembles for active learning in image classification. In [Proceedings of the IEEE Conference on Computer Vision and Pattern Recognition](#), pp. 9368–9377, 2018.

Chaloner, K. and Verdinelli, I. Bayesian experimental design: A review. [Statistical Science](#), pp. 273–304, 1995.

Christie, G., Fendley, N., Wilson, J., and Mukherjee, R. Functional map of the world. In [Proceedings of the IEEE Conference on Computer Vision and Pattern Recognition](#), pp. 6172–6180, 2018.

Gal, Y. and Ghahramani, Z. Dropout as a bayesian approximation: Representing model uncertainty in deep learning. In [international conference on machine learning](#), pp. 1050–1059. PMLR, 2016.

Gal, Y., Islam, R., and Ghahramani, Z. Deep bayesian active learning with image data. In International Conference on Machine Learning, pp. 1183–1192. PMLR, 2017.

Hartigan, J. Bounding the maximum of dependent random variables. Electronic Journal of Statistics, 8(2):3126–3140, 2014.

Kirsch, A., Rainforth, T., and Gal, Y. Test distribution-aware active learning: A principled approach against distribution shift and outliers. 2021.

Koh, P. W., Sagawa, S., Marklund, H., Xie, S. M., Zhang, M., Balsubramani, A., Hu, W., Yasunaga, M., Phillips, R. L., Gao, I., Lee, T., David, E., Stavness, I., Guo, W., Earnshaw, B. A., Haque, I. S., Beery, S., Leskovec, J., Kundaje, A., Pierson, E., Levine, S., Finn, C., and Liang, P. Wilds: A benchmark of in-the-wild distribution shifts. 2021.

Krizhevsky, A., Hinton, G., et al. Learning multiple layers of features from tiny images. 2009.

LeCun, Y. The mnist database of handwritten digits. <http://yann.lecun.com/exdb/mnist/>, 1998.

Lewis, D. D. and Gale, W. A. A sequential algorithm for training text classifiers. In SIGIR’94, pp. 3–12. Springer, 1994.

Lindley, D. V. On a measure of the information provided by an experiment. The Annals of Mathematical Statistics, pp. 986–1005, 1956.

Miller, J. P., Taori, R., Raghunathan, A., Sagawa, S., Koh, P. W., Shankar, V., Liang, P., Carmon, Y., and Schmidt, L. Accuracy on the line: on the strong correlation between out-of-distribution and in-distribution generalization. In International Conference on Machine Learning, pp. 7721–7735. PMLR, 2021.

Netzer, Y., Wang, T., Coates, A., Bissacco, A., Wu, B., and Ng, A. Y. Reading digits in natural images with unsupervised feature learning. 2011.

Rabanser, S., Günnemann, S., and Lipton, Z. Failing loudly: An empirical study of methods for detecting dataset shift. In Wallach, H., Larochelle, H., Beygelzimer, A., d’Alché-Buc, F., Fox, E., and Garnett, R. (eds.), Advances in Neural Information Processing Systems, volume 32. Curran Associates, Inc., 2019. URL <https://proceedings.neurips.cc/paper/2019/file/846c260d715e5b854ffad5f70a516c88-Paper.pdf>.

Roy, N. and McCallum, A. Toward optimal active learning through monte carlo estimation of error reduction. ICML, Williamstown, 2:441–448, 2001.

Schrouff, J., Harris, N., Koyejo, O., Alabdulmohsin, I., Schnider, E., Opsahl-Ong, K., Brown, A., Roy, S., Mincu, D., Chen, C., Dieng, A., Liu, Y., Natarajan, V., Karthikesalingam, A., Heller, K. A., Chiappa, S., and D’Amour, A. Maintaining fairness across distribution shift: do we have viable solutions for real-world applications? CoRR, abs/2202.01034, 2022. URL <https://arxiv.org/abs/2202.01034>.

Sener, O. and Savarese, S. Active learning for convolutional neural networks: A core-set approach. 2018.

Settles, B. Active learning literature survey. 2009.

Simonyan, K. and Zisserman, A. Very deep convolutional networks for large-scale image recognition. arXiv preprint arXiv:1409.1556, 2014.

Sinha, S., Ebrahimi, S., and Darrell, T. Variational adversarial active learning. 2019.

Tong, S. and Koller, D. Support vector machine active learning with applications to text classification. Journal of machine learning research, 2(Nov):45–66, 2001.

Virtanen, P., Gommers, R., Oliphant, T. E., Haberland, M., Reddy, T., Cournapeau, D., Burovski, E., Peterson, P., Weckesser, W., Bright, J., van der Walt, S. J., Brett, M., Wilson, J., Millman, K. J., Mayorov, N., Nelson, A. R. J., Jones, E., Kern, R., Larson, E., Carey, C. J., Polat, İ., Feng, Y., Moore, E. W., VanderPlas, J., Laxalde, D., Perktold, J., Cimrman, R., Henriksen, I., Quintero,

E. A., Harris, C. R., Archibald, A. M., Ribeiro, A. H., Pedregosa, F., van Mulbregt, P., and SciPy 1.0 Contributors. SciPy 1.0: Fundamental Algorithms for Scientific Computing in Python. *Nature Methods*, 17:261–272, 2020. doi: 10.1038/s41592-019-0686-2.

Welling, M. and Teh, Y. W. Bayesian learning via stochastic gradient langevin dynamics. In *Proceedings of the 28th international conference on machine learning (ICML-11)*, pp. 681–688. Citeseer, 2011.

Zhang, R., Li, C., Zhang, J., Chen, C., and Wilson, A. G. Cyclical stochastic gradient mcmc for bayesian deep learning. *arXiv preprint arXiv:1902.03932*, 2019.

Zhao, E., Liu, A., Anandkumar, A., and Yue, Y. Active learning under label shift. In *The 24th International Conference on Artificial Intelligence and Statistics, AISTATS 2021, April 13-15, 2021, Virtual Event*, volume 130 of *Proceedings of Machine Learning Research*, pp. 3412–3420. PMLR, 2021. URL <http://proceedings.mlr.press/v130/zhao21b.html>.

## A Appendix

### A.1 Log likelihood loss optimal prediction

In Section 3.1, it was noted that the optimal prediction probability  $a$  is  $\Pr(Y_j = \cdot | Y_i = y_i)$ . Let  $\vec{p} \in \Delta_C$  be the vector representation of  $\Pr(Y_j = \cdot | Y_i = y_i)$ ; in other words,  $\vec{p}_c = \Pr(Y_j = c | Y_i = y_i)$ . So,

$$\mathbb{E}_{y_j \sim Y_j | Y_i = y_i} [-\log a_{y_j}] = \sum_{c=1}^C \vec{p}_c (-\log a_c) \quad (9)$$

To show that  $a = \vec{p}$  is the optimal prediction, we must show its value is always equal or less than the value of any other  $a' \in \Delta_C$ . Note that the KL divergence is always non-negative,

$$\sum_{c=1}^C \vec{p}_c \log \left( \frac{\vec{p}_c}{a'_c} \right) \geq 0 \quad (10)$$

$$\sum_{c=1}^C \vec{p}_c (-\log a'_c) \geq \sum_{c=1}^C \vec{p}_c (-\log \vec{p}_c) \quad (11)$$

(12)

### A.2 Computational complexity

For MELL and MEZL, the amount of computation required for each candidate sample  $i$  and validation sample  $j$  is proportional to  $TC^2$ , where  $T$  is the number of posterior samples and  $C$  is the number of classes. Thus the leading order term in the active learning algorithm (not including the train time) is  $O(Kn_{\text{pool}}n_{\text{val}}TC^2)$ . We can decrease the computational complexity dependence on  $n_{\text{pool}}$  and  $n_{\text{val}}$  by subsampling at each active learning iteration. For BADGE (Ash et al., 2019), the main cost comes from the  $k$ -means++ algorithm run  $K$  times (once per active learning iteration) for a total computational cost of  $O(Kn_{\text{pool}}n_{\text{query}}d)$ , where  $d$  is the embedding dimension. Because  $d$  may be quite large, and we cannot subsample to reduce the dependence on  $n_{\text{query}}$ , the high computational cost of running BADGE might be expected.

### A.3 Experimental Details

#### A.3.1 Score Functions

Below, we have the scoring functions for the baseline methods.

**Entropy**, **Entropy\\_MC**, **BALD**, and **Random** assign each data sample  $i$  a score, and then query the labels of the samples with the top  $n_{query}$  scores.

Given a function `unif` that samples randomly from the uniform distribution over  $[0, 1]$ , **Random** has the following scoring function:

$$\text{Score}_i^{\text{Random}} = \text{unif}()$$

For **Entropy**:

$$\text{Score}_i^{\text{Entropy}} = - \sum_{c \in [C]} \Pr(Y_i = c|x_i, \theta^*) \log \Pr(Y_i = c|x_i, \theta^*)$$

where  $\theta^*$  is the trained model parameters.

For **Entropy\\_MC**:

$$\text{Score}_i^{\text{Entropy\_MC}} = - \sum_{c \in [C]} \Pr(Y_i = c|x_i, \mathcal{D}) \log \Pr(Y_i = c|x_i, \mathcal{D})$$

where

$$\Pr(Y_i = c|x_i, \mathcal{D}) \approx \frac{1}{T} \sum_{t=1}^T \Pr(Y_i = c|x_i, \theta_t)$$

For **BALD**:

$$\text{Score}_i^{\text{BALD}} = \text{Score}_i^{\text{Entropy\_MC}} + \frac{1}{T} \sum_{t=1}^T \left( \sum_{c \in [C]} \Pr(Y_i = c|x_i, \theta_t) \log \Pr(Y_i = c|x_i, \theta_t) \right)$$

**BADGE** and **Coreset** choose samples in batches.

For **BADGE** Ash et al. (2019), gradient embeddings are computed according to:

$$g_x = \frac{\partial}{\partial \theta_{\text{out}}} \ell_{\text{CE}}(f(x; \theta), \hat{y}(x))$$

where  $\theta_{\text{out}}$  is the model parameters at the last layer,  $f(x; \theta)$  is the output of model  $\theta$ , and  $\hat{y}(x)$  is the hypothetical label on  $x$ . The k-means++ seeding algorithm is then run on these gradient embeddings to choose samples.

**Coreset** seeks to solve the following problem:

$$\min_{B: |B| \leq n_{\text{query}}} \max_{i \in \mathcal{U}} \min_{j \in B \cup \mathcal{D}} \Delta(x_i, x_j)$$

In other words, choose a batch of  $n_{\text{query}}$  data samples, such that the maximum distance between data samples in the unlabeled set  $\mathcal{U}$  and their closest center is minimized. Since computing this is NP-Hard, a k-greedy center approach is first used to initialize batch  $B$ , and a mixed integer program is run as a sub-routine to iteratively approach the optimal Sener & Savarese (2018).

### A.3.2 Datasets

**CIFAR10** and **CIFAR100** (Krizhevsky et al., 2009) are standard image classification datasets. **SVHN** (Netzer et al., 2011) and **MNIST** (LeCun, 1998) are digit recognition datasets, with the former containing color data from house numbers and the latter with black and white handwritten digits. **iWildCam** (Beery et al., 2020), **Camelyon17** (Bandi et al., 2018), and **FMoW** (Christie et al., 2018) are drawn from the WILDS repository of datasets (Koh et al., 2021). **iWildCam** contains images of wildlife captured using camera traps around the world. **Camelyon17** contains microscope images of tissue samples taken from various patients, with the goal of identifying whether the image contains metastasized cancer cells. Finally, **FMoW** contains satellite imagery with the task of classifying the type of building or land represented in the image.

For each dataset, we conduct one experiment with and one experiment without data shift. In the no shift setting, the initial training (seed), validation, unlabeled, and test sets are drawn uniformly at random from the available data (we ignore train/test/validation splits that come from the dataset). In the data shift settings, we split the dataset into a source and a target set, where source and target come from different distributions. The initial training (seed) set is sampled uniformly at random from the

source set. The validation, unlabeled, and test sets are sampled uniformly at random from the target set.

We create the shift setting in CIFAR10, CIFAR100, SVHN, and MNIST by assigning the  $n_{seed}$  images with lowest average pixel brightness to the source and all other images in the dataset to the target set. Shifted settings for Camelyon17, iWildCam, and FMoW are naturally occurring in how the datasets were collected. Using their split columns in the metadata files, we assign splits  $\in \{0, 1\}$  for Camelyon17, splits  $\in \{\text{val, test}\}$  for iWildCam, and splits  $\in \{\text{train}\}$  for FMoW to the source set. We assign splits  $\in \{2, 3, 4\}$  for Camelyon17, splits  $\in \{\text{id\_val, id\_test, train}\}$  for iWildCam, and splits  $\notin \{\text{train}\}$  for FMoW to the target set.

### A.3.3 Experimental Parameters

In each experiment, we initialize our training (seed), validation, unlabeled, and test sets to  $n_{seed}$ ,  $n_{val}$ ,  $n_{pool}$ , and  $n_{test}$  samples respectively. At each active learning iteration, we train a task classifier with the VGG16 architecture (Simonyan & Zisserman, 2014) and an unweighted cross-entropy loss function. Then, an active learning method is used to query  $n_{query}$  samples from the unlabeled pool to label, adding them to the training set before the next iteration. We run each experiment 10 times with different random seeds. See Table 2 for details on task model training parameters and Table 3 for details on experiment parameters.

Table 2: A summary of hyperparameters used in our task model training. Note that the number of images processed during training (iterations multiplied by batch size) is 3000000. In the learning rate column, the number in parenthesis is the initial learning rate for SVHN and Camelyon and the number outside is the initial learning rate for all other datasets. The learning rate is divided by 10 every 11718 iterations.

Train Iterations	Batch Size	Learning Rate	Optimizer (Weight Decay, Momentum)	Loss
46875	64	0.01 (0.001)	SGD (5e-4, 0.9)	Cross-Entropy

Table 3: A summary of datasets and experimental setup parameters used in our experiments. For consistency, a two-pixel black border was added to MNIST to raise the image size from 28x28 to 32x32.  $|C|$  refers to the number of classes.  $L$  is the size of the subset sampled from the validation set to use in MELL and MEZL’s calculations.  $J$  is the size of the subset sampled from the unlabeled pool to use in MELL and MEZL’s calculations.  $T$  is the number of samples drawn from the posterior using Monte Carlo dropout in MELL, MEZL, Entropy MC, and BALD.

Dataset	Image Size	$ C $	Shift	$n_{seed}$	$n_{val}$	$n_{pool}$	$n_{query}$	$n_{test}$	$K$	$L$	$J$	$T$
CIFAR10	$32 \times 32$	10	None shift	5000 20000	5000 5000	40000 25000	2500 1000	10000 10000	16 20	100 100	25000 10000	100 100
CIFAR100	$32 \times 32$	100	None shift	5000 20000	5000 5000	40000 25000	2500 1000	10000 10000	16 20	100 100	25000 10000	100 100
SVHN	$32 \times 32$	10	None shift	5000 20000	5000 5000	50000 35000	2500 1000	10000 10000	20 20	100 100	25000 10000	100 100
MNIST	$32 \times 32$	10	None shift	200 200	5000 5000	44800 44800	80 80	10000 10000	10 10	100 100	800 800	100 100
Camelyon17	$96 \times 96$	2	None shift	5000 20000	5000 5000	100000 100000	2500 1000	10000 10000	20 20	100 100	25000 10000	100 100
iWildCam	$64 \times 64$	182	None shift	5000 20000	5000 5000	100000 100000	2500 1000	10000 10000	20 20	100 100	25000 10000	100 100
FMoW	$96 \times 96$	62	None shift	5000 20000	5000 5000	100000 97000	2500 1000	10000 10000	20 20	100 100	25000 10000	100 100

## A.4 Additional Results

### A.4.1 Full Results

Below, we show the active learning accuracy curves on all datasets with and without shift for all methods in Figure 3. We also show the area under the curve (AUC) of the accuracy curves in the no shift setting in Table 4 and with shift in Table 5.

Table 4: Area under the curve (AUC) of active learning accuracy curves for each method on datasets **without shift**. Cells contain mean AUC and standard deviation across 10 trials calculated using composite Simpson’s rule, as implemented in `scipy.integrate.simpson` (Virtanen et al., 2020). AUCs are normalized by the difference between the number of training samples at the last iteration and  $n_{\text{seed}}$ . “-” indicates that the experiment did not finish after 14 days.

Dataset (no shift)	MELL	MEZL	Random	BALD	Entropy MC	Entropy	Coreset	BADGE
CIFAR10	81.74	81.43	80.65	81.63	81.65	81.66	81.58	81.68
	$\pm 0.29$	$\pm 0.40$	$\pm 0.36$	$\pm 0.29$	$\pm 0.29$	$\pm 0.35$	$\pm 0.37$	$\pm 0.41$
CIFAR100	43.96	43.82	43.83	43.94	42.83	42.68	44.30	-
	$\pm 0.26$	$\pm 0.34$	$\pm 0.28$	$\pm 0.34$	$\pm 0.32$	$\pm 0.34$	$\pm 0.28$	
SVHN	91.73	91.48	90.41	91.75	91.80	91.80	91.71	91.80
	$\pm 0.15$	$\pm 0.15$	$\pm 0.12$	$\pm 0.12$	$\pm 0.15$	$\pm 0.14$	$\pm 0.15$	$\pm 0.15$
MNIST	97.50	96.71	96.23	97.10	97.27	97.28	97.35	97.60
	$\pm 0.11$	$\pm 0.27$	$\pm 0.28$	$\pm 0.18$	$\pm 0.20$	$\pm 0.19$	$\pm 0.17$	$\pm 0.18$
iWildCam	92.47	92.24	88.03	91.84	91.64	91.57	92.40	-
	$\pm 0.20$	$\pm 0.15$	$\pm 0.24$	$\pm 0.21$	$\pm 0.16$	$\pm 0.18$	$\pm 0.21$	
Camelyon17	98.02	97.06	97.02	98.12	98.11	98.13	97.28	98.12
	$\pm 0.10$	$\pm 0.19$	$\pm 0.10$	$\pm 0.09$	$\pm 0.11$	$\pm 0.10$	$\pm 0.10$	$\pm 0.11$
fMoW	36.43	36.43	35.10	36.48	34.90	34.75	36.67	-
	$\pm 0.44$	$\pm 0.35$	$\pm 0.33$	$\pm 0.46$	$\pm 0.44$	$\pm 0.38$	$\pm 0.33$	

Table 5: Area under the curve (AUC) of active learning accuracy curves for each method on each dataset **with shift**. Cells contain mean AUC and standard deviation across 10 trials calculated using composite Simpson’s rule, as implemented in `scipy.integrate.simpson` (Virtanen et al., 2020). AUCs are normalized by the difference between the number of training samples at the last iteration and  $n_{\text{seed}}$ . “-” indicates that the experiment did not finish after 14 days.

Dataset (shift)	MELL	MEZL	Random	BALD	Entropy MC	Entropy	Coreset	BADGE
CIFAR10	84.11	83.75	83.10	84.09	84.13	84.34	84.19	84.28
	$\pm 0.26$	$\pm 0.35$	$\pm 0.34$	$\pm 0.23$	$\pm 0.26$	$\pm 0.24$	$\pm 0.28$	$\pm 0.26$
CIFAR100	48.51	48.46	48.16	48.46	47.93	47.35	48.19	48.12
	$\pm 0.36$	$\pm 0.34$	$\pm 0.38$	$\pm 0.53$	$\pm 0.46$	$\pm 0.40$	$\pm 0.35$	$\pm 0.31$
SVHN	91.09	90.76	89.52	91.09	91.10	91.28	90.84	91.26
	$\pm 0.25$	$\pm 0.35$	$\pm 0.29$	$\pm 0.28$	$\pm 0.27$	$\pm 0.29$	$\pm 0.28$	$\pm 0.25$
MNIST	91.96	91.71	91.92	86.03	88.14	84.06	91.55	93.32
	$\pm 0.52$	$\pm 0.42$	$\pm 0.32$	$\pm 2.28$	$\pm 1.77$	$\pm 3.54$	$\pm 0.53$	$\pm 0.32$
iWildCam	85.17	85.22	79.84	80.14	78.92	76.54	83.37	-
	$\pm 0.33$	$\pm 0.37$	$\pm 0.32$	$\pm 0.32$	$\pm 0.39$	$\pm 1.11$	$\pm 0.47$	
Camelyon17	96.59	96.63	96.59	95.79	96.15	97.62	92.20	97.67
	$\pm 0.60$	$\pm 0.07$	$\pm 0.12$	$\pm 1.25$	$\pm 0.53$	$\pm 0.10$	$\pm 0.54$	$\pm 0.17$
fMoW	33.08	33.17	32.33	33.17	32.12	31.84	33.22	-
	$\pm 0.27$	$\pm 0.36$	$\pm 0.40$	$\pm 0.27$	$\pm 0.29$	$\pm 0.34$	$\pm 0.30$	

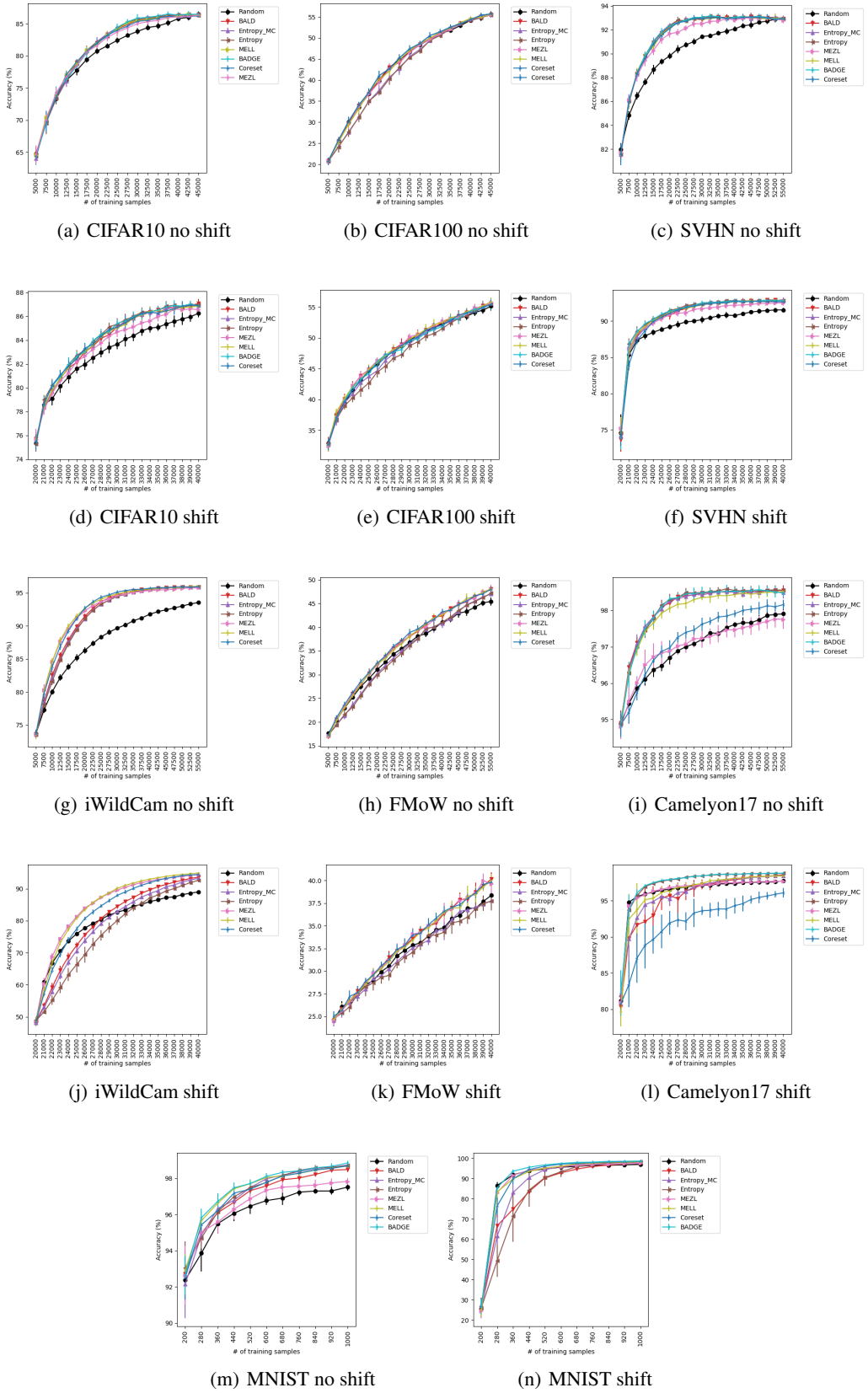


Figure 3: Active learning curves computed on the test set for all experiments.

#### A.4.2 Cyclical SG-MCMC Sampling Method

In this experiment, we compare using *Cyclical SG-MCMC* as our Bayesian sampling method against *Monte Carlo dropout*. We train all task models by *Cyclical SG-MCMC* proposed in Zhang et al. (2019). The initial step-size is  $\alpha_0 = 0.5$  and the number of cycles is  $M = 10$ . We collect 10 samples per cycle. Collected samples are used as the samples from posterior distribution in MELL\_MCMC. For all other methods, we use dropout to collect samples from the posterior distribution. According to the experiment, we did not observe any significant improvement to using *Cyclical SG-MCMC* compared to *drop-out* in the active learning context.

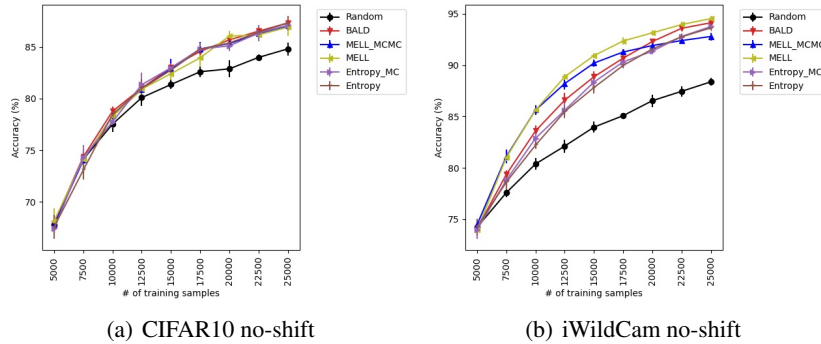


Figure 4: Cyclical SG-MCMC is used in training all methods. Posterior samples are generated by Monte Carlo dropout for all methods, except MELL\_MCMC, for which we use samples from "sampling phase" in Cyclical SG-MCMC. In both experiments, we used datasets without data shift.

#### A.5 General Bayesian active learning guarantees

To the best of our knowledge, finding a computationally efficient (polynomial-time) algorithm with guarantees for the model-free Bayesian active learning setting is an open challenge. All Bayesian active learning algorithms mentioned here (MELL, MEZL, BALD, Entropy) are myopic, in that they are motivated by the best decision if the budget only allowed for a single query, and have clear failure modes. In particular consider the following simple distribution over 100 pool samples and one validation sample. That is  $\forall i \in [100] : Y_i \sim U(\{0, 1\})$ , and  $Y_{\text{val}} = Y_1 \text{ XOR } Y_2$ .

Suppose we wish to predict  $Y_{\text{val}}$  by querying a subset of  $\{Y_i\}_{i=1}^{100}$ . In this case, the optimal strategy is to query  $Y_1$  and  $Y_2$  from which we can compute  $Y_{\text{val}}$ . However, existing algorithms value all possible queries equally. Because each  $Y_i$  has the same distribution, uncertainty sampling with entropy will behave randomly. If we set the parameters  $\theta$  for BALD to be the joint distribution, conditioning on any single variable decreases the entropy slightly, but by the same amount for each query. MEZL and MELL will also behave randomly because no query by itself gives any information about  $Y_{\text{val}}$ .

An algorithm based on planning ahead by two queries will behave optimally for this task, but at a large computational burden. Furthermore, planning ahead by two queries will fail for a slightly more difficult distribution, such as the case where  $Y_{\text{val}} = Y_1 \text{ XOR } Y_2 \text{ XOR } Y_3$ . More generally, if an algorithm only examines  $k$ -wise marginals of the labeling distribution, we can always construct a distribution such that all queries appear equal to the algorithm, but the optimal strategy only requires  $k + 1$  queries to remove all uncertainty about the validation set.

Designing a non-myopic strategy with guarantees remains an interesting area for future research. We can extend expected error reduction to the batching scenario with the log likelihood loss. We wish to find a batch  $B$  of size at most  $k$  that maximizes:

$$\max_{\substack{B \subset \mathcal{D}_{\text{pool}} \\ |B| \leq k}} f(B) = \sum_{v \in V} H(Y_v | Y_B) \quad (13)$$

It is straightforward to show that

$$f(B) = \sum_{v \in \mathcal{D}_{\text{val}}} \mathbb{E}_{\vec{a}} \left[ \sum_{c \in C} \frac{\Pr(Y_B = \vec{a}, Y_v = c)}{\Pr(Y_B = \vec{a})} \log \frac{\Pr(Y_B = \vec{a}, Y_v = c)}{\Pr(Y_B = \vec{a})} \right]$$

It is possible to estimate  $f(B)$  via Monte Carlo dropout. However, optimization 13 is NP and  $f(B)$  is not a sub-modular. Therefore, finding an efficient approximation algorithm for 13 needs further investigation.

### A.6 Analysis of MELL for Bayesian Linear Model

Consider the simple Bayesian linear model. Here,  $y = \theta^T x + \epsilon$  is a multivariate normal distribution where  $\theta \sim \mathcal{N}(\mu_\theta, \Sigma_\theta)$  and  $\epsilon \sim \mathcal{N}(0, \sigma^2)$  and  $\mu_\theta \in \mathbb{R}^d$ ,  $\Sigma_\theta \in \mathbb{R}^{d \times d}$ , and assume that  $\Sigma_\theta$  is positive-definite. For a given sample  $x$ , the distribution of its label is

$$Y_x \sim \mathcal{N}(\mu_\theta^T x, x^T \Sigma_\theta x + \sigma^2).$$

Therefore,

$$H[Y_x] = \frac{1}{2} \log(2\pi e) + \frac{1}{2} \log(x^T \Sigma_\theta x + \sigma^2).$$

Then, we have

$$I(Y_x, \theta) = H[Y_x] - E[H[Y_x | \theta]] = \frac{1}{2} \log(x^T \Sigma_\theta x + \sigma^2) - \frac{1}{2} \log(\sigma^2). \quad (14)$$

**BALD** selects the samples with highest mutual information between model parameters and the label of the sample. Therefore, BALD chooses the samples with highest  $x^T \Sigma_\theta x$  for  $x \in \mathcal{D}_{\text{pool}}$ . This criterion is known in Bayesian Experimental Design literature; for instance Chaloner & Verdinelli (1995). Assume that the samples in pool  $\mathcal{D}_{\text{pool}}$  is drawn from a continuous unbounded data distribution, then  $\max_{x \in \mathcal{D}_{\text{pool}}} x^T \Sigma_\theta x \rightarrow \infty$  as  $n_{\text{pool}} \rightarrow \infty$  where  $n_{\text{pool}} = |\mathcal{D}_{\text{pool}}|$ . For instance, if the underlying distribution for the pool data set is Gaussian then we can use the properties of the maxima of Gaussian distribution in Hartigan (2014) and show that<sup>†</sup>

$$\max_{x \in \mathcal{D}_{\text{pool}}} x^T \Sigma_\theta x = \Theta(\log(n_{\text{pool}}))$$

which implies that if  $x^*$  is the selected sample by BALD, then  $\|x^*\| \rightarrow \infty$  as  $n_{\text{pool}} \rightarrow \infty$ .

**MELL** selects the samples with highest mutual information between the sample's label and the labels of the validation set. Let  $x$  be the candidate sample and  $v$  is a sample drawn from validation set with corresponding labels  $Y_x$  and  $Y_v$ . The labels for these two samples are jointly Gaussian and one can easily show that  $\text{Var}(Y_x) = x^T \Sigma_\theta x + \sigma^2$ ,  $\text{Var}(Y_v) = v^T \Sigma_\theta v + \sigma^2$  and  $\text{cov}(Y_x, Y_v) = x^T \Sigma_\theta v$ . So the correlation between these two r.v. can be derived by

$$r(x, v) = \text{Corr}(Y_x, Y_v) = \frac{x^T \Sigma_\theta v}{\sqrt{(x^T \Sigma_\theta x + \sigma^2)(v^T \Sigma_\theta v + \sigma^2)}} \quad (15)$$

Using the mutual information formula for jointly-Gaussian distribution, we can show that

$$E_v[I(Y_x, Y_v)] = \frac{-1}{2} E_v \left[ \log \left( 1 - r(x, v)^2 \right) \right] \quad (16)$$

For small enough  $\frac{\Sigma_\theta}{\sigma^2} \ll 1$ ,

$$E_v[I(Y_x, Y_v)] \approx \frac{1}{2} E_v[r(x, v)^2]$$

Therefore, MELL selects the most correlated samples with the validation set, in contrast to BALD which is selecting samples with the largest norm.

Recall from decomposition 7, we have

$$I(Y_x; \theta) = I(Y_x; Y_v) + I(Y_x; \theta | Y_v). \quad (17)$$

In the next proposition, we show that the first term of right hand side is bounded and the second term goes to infinity for large enough  $\|x\|_\theta^2 = x^T \Sigma_\theta x$ . As we mentioned earlier, the selected samples by BALD  $\|x_i^*\| \rightarrow \infty$  as  $|\mathcal{D}_{\text{pool}}| \rightarrow \infty$  if  $\mathcal{D}_{\text{pool}}$  are drawn from an unbounded distribution. So the irreverent information term (second term) in decomposition 17 dominants the BALD sampling objective and thus samples with the largest norm are selected. In contrast, the MELL objective is the relevant mutual information (first term) in decomposition 17, thus it is not confused by samples from the pool with large magnitude.

---

<sup>†</sup>Here,  $f(x) = \Theta(g(x))$  means that there exists positive constants  $c_1, c_2$  and  $x_0$  such that  $c_1 g(x) \leq f(x) \leq c_2 g(x)$  for all  $x \geq x_0$ .

**Proposition 1.** Let  $Y = \theta x + \epsilon$  be a linear Bayesian model where  $\theta \sim \mathcal{N}(\mu_\theta, \Sigma_\theta)$  and  $\epsilon \sim \mathcal{N}(0, \sigma^2)$  are independent. Then, there exists constant  $C$  such that

$$E_v[I(Y_x; Y_v)] \leq C.$$

for all  $x \in \mathcal{D}_{pool}$ . Furthermore,  $E_v[I(Y_x; \theta|Y_v)] = \Theta(\log(x^T \Sigma_\theta x))$  for large enough  $x$ .

**Remark.** We show that

$$C = \frac{1}{2\sigma^2} E_v[v^T \Sigma_\theta v]$$

*Proof.* Given that  $Y_x = \theta^T x + \epsilon$  and  $Y_v = \theta^T v + \epsilon'$ , we have

$$\begin{aligned} \text{Var}(\alpha Y_x - Y_v) &= \text{Var}((\alpha \epsilon - \epsilon') + \theta^T(\alpha x - v)) \\ &\geq \sigma^2(1 + \alpha^2) \geq \sigma^2 \end{aligned} \tag{18}$$

for every  $\alpha \in \mathbb{R}$ . Here we use the independence assumption between parameters and noise. Letting  $\alpha = \frac{\text{cov}(Y_x, Y_v)}{\text{Var}(Y_x)}$ , observe that

$$\begin{aligned} \text{Var}(\alpha Y_x - Y_v) &= \alpha^2 \text{Var}(Y_x) - 2\alpha \cdot \text{cov}(Y_x, Y_v) + \text{Var}(Y_v) \\ &= \frac{\text{cov}(Y_x, Y_v)^2}{\text{Var}(Y_x)} - 2 \frac{\text{cov}(Y_x, Y_v)}{\text{Var}(Y_x)} \cdot \text{cov}(Y_x, Y_v) + \text{Var}(Y_v) \\ &= \text{Var}(Y_v) - \frac{\text{cov}(Y_x, Y_v)^2}{\text{Var}(Y_x)} \end{aligned}$$

Using Inequality 18, we can conclude that

$$\text{Var}(Y_v) - \frac{\text{cov}(Y_x, Y_v)^2}{\text{Var}(Y_x)} \geq \sigma^2$$

Observe that  $\text{Var}(Y_x) = x^T \Sigma_\theta x + \sigma^2$ ,  $\text{Var}(Y_v) = v^T \Sigma_\theta v + \sigma^2$  and  $\text{cov}(Y_x, Y_v) = x^T \Sigma_\theta v$ . Thus,

$$1 - r(x, v)^2 = 1 - \frac{\text{cov}(Y_x, Y_v)^2}{\text{Var}(Y_x) \text{Var}(Y_v)} \geq \frac{\sigma^2}{\text{Var}(Y_v)}$$

Taking log from both sides and using the fact that  $\log z > 1 - 1/z$ , we have

$$\log(1 - r(x, v)^2) \geq \log\left(\frac{\sigma^2}{\sigma^2 + v^T \Sigma_\theta v}\right) > 1 - \frac{1}{\sigma^2}(\sigma^2 + v^T \Sigma_\theta v) = -\frac{1}{\sigma^2}(v^T \Sigma_\theta v)$$

By taking the expectation and using Equation 16, we can conclude that

$$E_v[I(Y_x; Y_v)] < C = \frac{1}{2\sigma^2} E_v[v^T \Sigma_\theta v]$$

for all  $x \in \mathcal{D}_{pool}$ . The second part of the proposition is a direct result of decomposition 17 and the observation that  $I(Y_x, \theta) = \Theta(\log(x^T \Sigma_\theta x))$  for linear model.  $\square$